

# UC Berkeley

## UC Berkeley Previously Published Works

### Title

Record High Single-Ion Magnetic Moments Through 4f n 5d1 Electron Configurations in the Divalent Lanthanide Complexes [(C<sub>5</sub>H<sub>4</sub>SiMe<sub>3</sub>)<sub>3</sub>Ln]–

### Permalink

<https://escholarship.org/uc/item/4c1473cs>

### Journal

Journal of the American Chemical Society, 137(31)

### ISSN

0002-7863

### Authors

Meihaus, Katie R  
Fieser, Megan E  
Corbey, Jordan F  
[et al.](#)

### Publication Date

2015-08-12

### DOI

10.1021/jacs.5b03710

Peer reviewed

# Record High Single-Ion Magnetic Moments Through $4f^n5d^1$ Electron Configurations in the Divalent Lanthanide Complexes $[(C_5H_4SiMe_3)_3Ln]^-$

Katie R. Meihaus,<sup>†</sup> Megan E. Fieser,<sup>‡</sup> Jordan F. Corbey,<sup>‡</sup> William J. Evans,<sup>\*,‡</sup> and Jeffrey R. Long<sup>\*,†,§</sup>

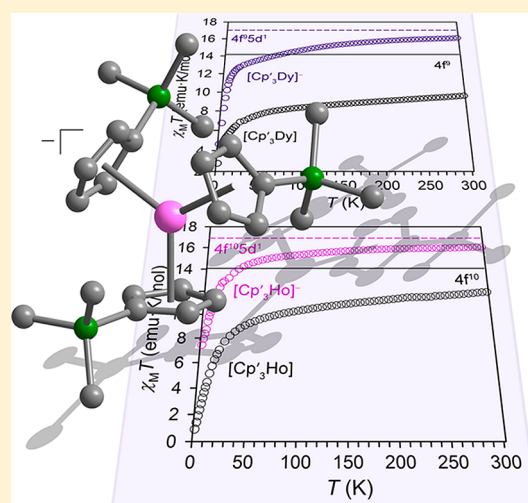
<sup>†</sup>Department of Chemistry, University of California, Berkeley, California 94720, United States

<sup>‡</sup>Department of Chemistry, University of California, Irvine, California 92697, United States

<sup>§</sup>Materials Science Division, Lawrence Berkeley National Laboratory, Berkeley, California 94720, United States

## Supporting Information

**ABSTRACT:** The recently reported series of divalent lanthanide complex salts, namely  $[K(2.2.2\text{-cryptand})][Cp'_3Ln]$  ( $Ln = Y, La, Ce, Pr, Nd, Sm, Eu, Gd, Tb, Dy, Ho, Er, Tm$ ;  $Cp' = C_5H_4SiMe_3$ ) and the analogous trivalent complexes,  $Cp'_3Ln$ , have been characterized via dc and ac magnetic susceptibility measurements. The salts of the complexes  $[Cp'_3Dy]^-$  and  $[Cp'_3Ho]^-$  exhibit magnetic moments of 11.3 and 11.4  $\mu_B$ , respectively, which are the highest moments reported to date for any monometallic molecular species. The magnetic moments measured at room temperature support the assignments of a  $4f^{n+1}$  configuration for  $Ln = Sm, Eu, Tm$  and a  $4f^n5d^1$  configuration for  $Ln = Y, La, Gd, Tb, Dy, Ho, Er$ . In the cases of  $Ln = Ce, Pr, Nd$ , simple models do not accurately predict the experimental room temperature magnetic moments. Although an *LS* coupling scheme is a useful starting point, it is not sufficient to describe the complex magnetic behavior and electronic structure of these intriguing molecules. While no slow magnetic relaxation was observed for any member of the series under zero applied dc field, the large moments accessible with such mixed configurations present important case studies in the pursuit of magnetic materials with inherently larger magnetic moments. This is essential for the design of new bulk magnetic materials and for diminishing processes such as quantum tunneling of the magnetization in single-molecule magnets.



## INTRODUCTION

The study of magnetic materials continues to drive research in chemistry and physics, in particular permanent magnets and single-molecule magnets.<sup>1</sup> Certainly, these two categories differ vastly in size, composition, operating temperatures, and current applications.<sup>1</sup> While permanent magnets are currently used in areas ranging from wind turbines to electric car motors,<sup>2</sup> single-molecule magnets still represent an exploratory area of chemistry and physics research. Additionally, permanent magnets based on synthetic lanthanide-containing systems, such as  $Nd_2Fe_{14}B^3$  and  $SmCo_5$ ,<sup>4</sup> derive their properties from the coupling of the anisotropic lanthanide moments with itinerant electrons contributed by the diffuse 3d metal orbitals. On the other hand, single-molecule magnets are often composed of only several magnetic centers or a single metal ion surrounded by an appropriate ligand field and exhibit magnetic hysteresis below 14 K.<sup>5</sup> While magnetic coupling has led to some truly exceptional systems,<sup>6</sup> fine-tuning the ligand field around a particular magnetic ion is the predominant means through which the magnetic properties of these molecules can be modulated.<sup>5a-c</sup>

A key connection between these two categories of materials is the importance of the lanthanide ions in engendering extraordinary properties. Indeed, the hardness of both permanent magnets and single-molecule magnets stems from the significant magnetic anisotropy of the lanthanide ions, originating from strong spin-orbit coupling and the core-like nature of the 4f orbitals. Another important contribution from the lanthanide centers is their inherently large magnetic moments arising from large total angular momentum *J* ground states. In the case of permanent magnets, large lanthanide anisotropy and magnetic moments enhance such properties as the coercive field and saturation magnetization, both of which influence the amount of useful work that can be achieved with a given material. For single-molecule magnets, lanthanide magnetic anisotropy in the presence of a suitable crystal field can enhance hysteresis temperature, while a larger magnitude *J* ground state can diminish ground-state tunneling,<sup>7</sup> leading to

Received: April 9, 2015

Published: July 13, 2015

wider hysteresis loops and hence larger coercivity in molecular materials.

In designing new bulk magnets (e.g., Dy<sup>III</sup> in Nd<sub>2</sub>Fe<sub>14</sub>B<sup>8</sup>) and single-molecule magnets, electronic modification is made primarily through dopant atoms or symmetry and ligand field alterations. These alterations may enhance the magnetic anisotropy, though another important parameter, namely the overall magnetic moment for the material, cannot be substantially altered without changing the identity of the constituent metals. It is interesting to consider how current properties of lanthanide-based magnetic materials may be further improved beyond tuning the crystal field surroundings, for instance by intrinsically enhancing the magnetic moment of one or more of the metal ions.

In this light, the recent discovery of the divalent state across the entire lanthanide series in compounds of the type [K(2.2.2-cryptand)][Cp'<sub>3</sub>Ln] (Cp' = C<sub>5</sub>H<sub>4</sub>SiMe<sub>3</sub>, Figure 1)<sup>9</sup> presents a

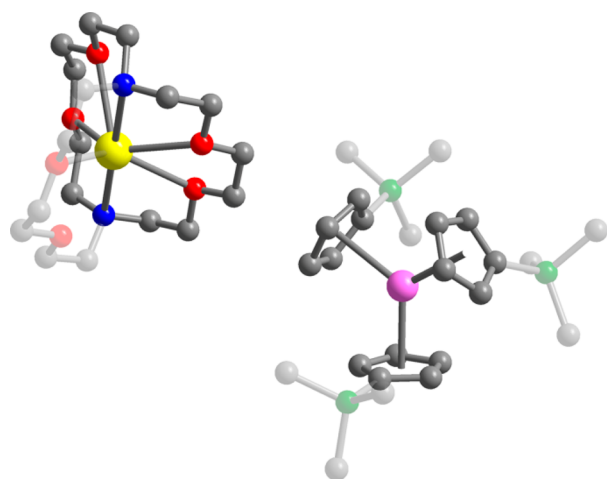


**Figure 1.** Crystal structure of [K(2.2.2-cryptand)][Cp'<sub>3</sub>Ho]; pink, gray, green, yellow, red, and blue spheres represent Ho, C, Si, K, O, and N, respectively.<sup>7</sup> A molecule of THF that crystallizes in the lattice is not shown.

fascinating case study in the consideration of new magnetic centers for the design of exceptional new magnetic materials. Indeed, characterization via X-ray crystallography,<sup>10</sup> UV-vis spectrophotometry, and electronic structure calculations

suggests that in the cases of Ln = La, Ce, Pr, Nd, Gd, Tb, Dy, Ho, Er, Lu, the electronic configuration is an unprecedented 4f<sup>n</sup>5d<sup>1</sup>, wherein the d<sub>z<sup>2</sup></sub> orbital is preferentially occupied in the tris(cyclopentadienyl) ligand field.<sup>9</sup> In principle, the accessibility of this configuration should lead to larger magnetic moments, as the additional electron can enhance spin and also total angular momentum, *J*, in particular for the later lanthanides. An increase in the magnitude of the *J* ground state would lead to a concomitant increase in the overall magnetic moment compared to the trivalent lanthanides, which currently exhibit the highest magnetic moments for any metal ion. We report here the results of static and dynamic magnetic susceptibility measurements on the compounds [K(2.2.2-cryptand)][Cp'<sub>3</sub>Ln] (Figure 1) and their corresponding trivalent analogues Cp'<sub>3</sub>Ln and discuss the relevance of these results to the potential design of new magnetic materials.

## EXPERIMENTAL SECTION

The compounds [K(2.2.2-cryptand)][Cp'<sub>3</sub>Ln] and Cp'<sub>3</sub>Ln were prepared as previously reported.<sup>9</sup> Crystals of [K(2.2.2-cryptand)][Cp'<sub>3</sub>Ln] were grown from the THF reaction solution layered with Et<sub>2</sub>O at -35 °C, while crystals of Cp'<sub>3</sub>Ln were grown from pentane at -35 °C.

**Magnetic Measurements.** Magnetic samples were prepared by adding the powdered crystalline compound to a 5 mm inner diameter quartz tube with a quartz platform 3/4 down the length of the tube. For all samples but [K(2.2.2-cryptand)][Cp'<sub>3</sub>Ho], solid eicosane was added to prevent crystallite torquing and provide good thermal contact between the sample and the bath. The tubes were fitted with Teflon sealable adapters, evacuated using a glovebox vacuum pump, and flame-sealed under static vacuum. Following flame sealing, the solid eicosane was melted in a water bath held at 40 °C. Due to the previously observed temperature sensitivity of a number of these compounds, test samples were also prepared using cotton or Nujol (liquid at room temperature) as a restraint, to observe any effect of heating on the room temperature  $\chi_M T$  values. Static magnetic susceptibility data of such samples of Tm<sup>II</sup> (cotton), Dy<sup>II</sup> (nujol), and Nd<sup>II</sup> (cotton) exhibited significant magnetic torquing below 40 K, obscuring the low-temperature magnetic behavior. Even still, at high temperatures it was found that the moments of these samples agreed with those measured with eicosane restraint, and thus temperature-sensitivity was not a significant factor. In the case of Ho<sup>II</sup>, a sample firmly restrained with a small piece of cotton (no heating) did exhibit a slightly larger value of the static magnetic susceptibility times temperature ( $\chi_M T$ ) at 300 K (16.06 emu·K/mol for the cotton

**Table 1. Experimental and Predicted  $\chi_M T$  Values for the Ln<sup>II</sup> Complexes [Cp'<sub>3</sub>Ln]<sup>-</sup> and Ln<sup>III</sup> Complexes Cp'<sub>3</sub>Ln**

Ln <sup>II</sup>	<i>n</i>	exp. $\mu_{\text{eff}}^a$	exp. $\chi_M T^b$	$\chi_M T$ (4f <sup>n</sup> 5d <sup>1</sup> ) coupled	$\chi_M T$ (4f <sup>n+1</sup> )	$\chi_M T$ (4f <sup>n</sup> 5d <sup>1</sup> ) uncoupled	exp. (theor.) $\chi_M T$ Ln <sup>III</sup> (4f <sup>n</sup> )
Y	0	1.78	0.4	0.375	N/A	0.375	0
La	0	1.72	0.37	0.375	0.8	0.375	0
Ce	1	2.62	0.86	0.33	1.6	1.18	0.68 (0.8)
Pr	2	2.93	1.07	0.875	1.64	1.98	1.32 (1.6)
Nd	3	3.01	1.13	0.9	0.9	2.02	1.27 (1.64)
Sm	5	3.64	1.66	0	0	0.47	0.27 (0.09)
Eu	6	7.65	7.60	1.5	7.88	0.375	3.17 (0)
Gd	7	8.91	9.93	10	11.82	8.26	7.58 (7.88)
Tb	8	10.48	13.73	14.42	14.13	12.20	9.34 (11.82)
Dy	9	11.35	16.1	17.01	14.07	14.51	12.28 (14.13)
Ho	10	11.41	16.26	16.9	11.48	14.45	11.95 (14.07)
Er	11	9.94	12.35	14.06	7.15	11.86	11.35 (11.48)
Tm	12	4.14	2.22	9.23	2.57	7.53	6.38 (7.15)
Yb	13	0	0	3.9	0	2.95	2.42 (2.57)

<sup>a</sup>Units of  $\mu_B$ . <sup>b</sup>All  $\chi_M T$  data are reported in units of emu·K/mol and were collected under a field of 0.1 T (1 T in the case of Y<sup>II</sup> and La<sup>II</sup>).

sample versus 15.61 emu·K/mol for the eicosane sample). Thus, the reported Ho<sup>II</sup> data are from the sample restrained with cotton, while for all other compounds the data were obtained from eicosane-restrained samples.

Magnetic susceptibility measurements were performed using a Quantum Design MPMS2 SQUID magnetometer. Dc susceptibility data measurements were performed at temperatures ranging from 1.8 to 300 K, using applied fields of 1, 0.5, and 0.1 T (variable temperature) and fields ranging from 0 to 7 T (magnetization measurements, 2, 6, and 10 K). Ac magnetic susceptibility measurements were performed using a 4 Oe switching field. All data were corrected for diamagnetic contributions from the core diamagnetism estimated using Pascal's constants.<sup>11</sup>

## RESULTS AND DISCUSSION

Dynamic magnetic susceptibility measurements performed on Cp<sub>3</sub>Tb and Cp<sub>3</sub>Dy and all the divalent complexes<sup>12</sup> revealed only noise or high-frequency tails under zero or applied fields, indicating fast relaxation times and precluding the extraction of any information regarding a barrier to slow magnetic relaxation. Thus, no further exploration of the dynamic properties was carried out. In the case of the anisotropic trivalent lanthanide species, static magnetic susceptibility measurements revealed fairly characteristic temperature dependence, namely a relatively gradual decline of the  $\chi_M T$  product (and therefore also  $\mu_{\text{eff}} = \sqrt{8\chi_M T}$ ) with decreasing temperature, resulting from the presence of magnetic anisotropy and depopulation of the crystal field levels of the *J* ground state. For all lanthanides but Sm<sup>III</sup> and Eu<sup>III</sup>, the room temperature  $\chi_M T$  values are lower than those predicted for the free Ln<sup>3+</sup> ion (Figure S1 and Table 1), a result that has been observed previously for tris-(cyclopentadienyl) complexes.<sup>13</sup> These lower values can be ascribed to the size of the crystal field splitting, such that at room temperature the full *J* manifold is not completely populated. However, for Er<sup>III</sup>, Tm<sup>III</sup>, and Yb<sup>III</sup>, the  $\chi_M T$  values at 300 K very closely approach those determined for the respective free ions. In the case of Sm<sup>III</sup> and Eu<sup>III</sup>, the room temperature  $\chi_M T$  values are 0.27 and 3.17 emu·K/mol, respectively, substantially larger than the values of 0.09 and 0 emu·K/mol predicted for the free ions. This is a common result due to the presence of low-lying *J* = 7/2 (Sm<sup>III</sup>,  $\Delta$  = 1000 cm<sup>-1</sup>) and *J* = 1 (Eu<sup>III</sup>,  $\Delta$  = 300 cm<sup>-1</sup>) excited states for these ions, which renders the simple *LS* coupling scheme insufficient to describe the level population as the temperature is increased and  $k_B T$  exceeds  $\Delta$ .<sup>14</sup> In the case of the isotropic Gd<sup>III</sup> ion, the  $\chi_M T$  data are more or less linear over the entire temperature range from 300 to 1.8 K.

For nearly all of the divalent lanthanide complexes there is a substantial increase in the room temperature  $\chi_M T$  value when compared with the trivalent analogues, with the exception of Pr<sup>II</sup>, Nd<sup>II</sup>, and Tm<sup>II</sup>, which all exhibit smaller room temperature  $\chi_M T$  values than predicted even for the trivalent lanthanide ions (Table 1). To approach the analysis of the magnetic susceptibility for each complex, we can turn first to the ground electronic configurations suggested from experiment and theory;<sup>9</sup> namely, Eu<sup>II</sup> (Figure 2), Sm<sup>II</sup>, and Tm<sup>II</sup> (Figure S2) appear to fall into the 4f<sup>*n*+1</sup> category, while the remaining lanthanides lie in the 4f<sup>*n*</sup>5d<sup>1</sup> category.<sup>15</sup> For the former ions, this oxidation state is well-established in the literature,<sup>16</sup> and their ground electronic state may be described to a first approximation using *LS* coupling. For example, free Eu<sup>II</sup> with a 4f<sup>7</sup> configuration (*n* = 7, *L* = 0, *S* = 7/2) is predicted to exhibit  $\chi_M T$  = 7.88 emu·K/mol at room temperature, according to eq 1:

$$\chi_M T = g_J^2 J(J + 1)/8 \quad (1)$$

Indeed, the room temperature experimental  $\chi_M T$  value is 7.60 emu·K/mol for [K(2.2.2-cryptand)][Cp<sub>3</sub>Eu] (Figure 2, open light-blue circles), supporting the 4f<sup>7</sup> assignment for Eu<sup>II</sup>, as does the nearly temperature-independent behavior characteristic of an isotropic ion.

*LS* coupling provides a similarly reasonable description of the  $\chi_M T$  value at 300 K for Tm<sup>II</sup>, with the experimental value of 2.22 emu·K/mol agreeing quite well with the predicted value of 2.57 emu·K/mol. In the case of Sm<sup>II</sup>, a glance at the  $\chi_M T$  data reveals that *LS* coupling falls short, as was true above for Sm<sup>III</sup>. Indeed, the experimental  $\chi_M T$  value at 300 K is 1.66 emu·K/mol, while that predicted for 4f<sup>6</sup> is 0 emu·K/mol. Again, this result is suggestive of a low-lying *J* excited state, which is not uncommon for Sm<sup>II</sup>.<sup>17</sup>

For the lanthanides that were found to fall into the 4f<sup>*n*</sup>5d<sup>1</sup> category, a basic description of their ground states can be achieved using *LS* coupling rules. Given the indication from density functional theory (DFT) calculations that the added electron occupies the d<sub>z<sup>2</sup></sub> orbital,<sup>9</sup> the analysis can be simplified since this added electron would then contribute no orbital angular momentum. There are, however, two general possibilities we can consider regarding the nature of the coupling between the d electron, the f electrons, and the orbital angular momentum contributed by the latter. In particular, we can imagine a scenario where spin–spin coupling between the f and d electrons is stronger than any *LS* coupling, and thus we can describe the complexes with an overall spin of *S*<sub>TOT</sub> = *S*<sub>4f</sub> + 1/2. This total spin would then couple with the orbital angular

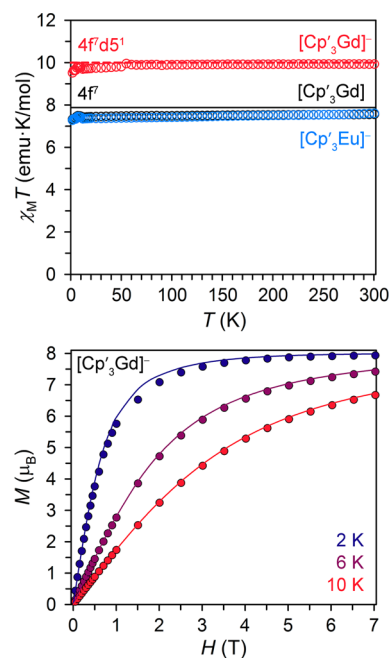


**Figure 2.** (Top) Plot of the static magnetic susceptibility times temperature ( $\chi_M T$ ) versus *T* collected at 0.1 T for [K(2.2.2-cryptand)][Cp<sub>3</sub>Ln] (Ln = Gd, red circles, Eu; light-blue circles) and the trivalent Cp<sub>3</sub>Gd (black circles). Dashed and solid lines represent the theoretical  $\chi_M T$  value at 300 K assuming the coupled 4f<sup>7</sup>5d<sup>1</sup> configuration for Gd<sup>II</sup> and the 4f<sup>7</sup> configuration for Gd<sup>III</sup>/Eu<sup>II</sup>, respectively. (Bottom) Variable-temperature *M*(*H*) curves for [K(2.2.2-cryptand)][Cp<sub>3</sub>Gd] collected from 0 to 7 T. Data points are given by colored spheres, and solid lines represent the corresponding Brillouin function for an *S* = 4 system.

momentum contributed by the f electrons, yielding an overall  $J$ , and then, using eq 1, we would arrive at theoretical  $\chi_M T$  values for a given lanthanide.

The alternative scenario is then one in which the  $LS$  coupling of the f electrons dominates (in general, where the d electron precesses with the magnetic field independently of the f electrons), and then the resulting  $\chi_M T$  value for the d electron ( $\chi_M T = 0.375$  emu·K/mol for  $S = 1/2$ ) would add to the  $\chi_M T$  value obtained for  $LS$  coupling for the f electrons. In other words, by adding 0.375 emu·K/mol to the theoretical  $\chi_M T$  value for a given  $\text{Ln}^{\text{III}}$ , one arrives at the predicted  $\text{Ln}^{\text{II}}$   $\chi_M T$  value and magnetic moment. In the following analysis, this latter scenario, where  $LS$  coupling  $\gg$  f electron spin coupling, will be referred to as the uncoupled scheme. The case described in the previous paragraph, now with f and d spin coupling  $\gg$   $LS$  coupling, will be referred to as the coupled scheme. This type of analysis was first introduced by Cloke and co-workers<sup>18</sup> in their discussion of the magnetism of zerovalent bis(1,3,5-*tert*-butylbenzene) lanthanide complexes. This earlier work is the motivation behind our present evaluation (as a brief aside we note that the possibility of a multiconfigurational ground state can also not be ruled out for some of these molecules, see below in the discussion for  $\text{Nd}^{\text{II}}$ , etc.). To investigate these two possibilities, the simplest lanthanide ion to start with is  $\text{Gd}^{\text{II}}$ , which should remain isotropic with the addition of an electron into an orbital of primarily  $d_z^2$  character. Indeed, the static magnetic susceptibility for  $[\text{K}(2.2.2\text{-cryptand})][\text{Cp}'_3\text{Gd}]$  collected under an applied field of 0.1 T over the temperature range from 1.8 to 300 K reveals a nearly temperature-independent  $\chi_M T$  product, with a room temperature magnitude of 9.93 emu·K/mol ( $\mu_{\text{eff}} = 8.91 \mu_B$ ) (Figure 2). Both of these factors support a  $4f^9 5d^1$  assignment, as a  $4f^{n+1}$  configuration should exhibit a  $\chi_M T$  product at room temperature much closer to the theoretical value of 11.82 emu·K/mol and should further show evidence of magnetic anisotropy, due to the  $J = 6$  ground state for a  $4f^8$  ion.

To address the nature of the interaction between the f electrons and the d electron, variable-field magnetization measurements were performed at temperatures of 2, 6, and 10 K (Figure 2). The data overlay quite well with the theoretical magnetization curves defined by an  $S = 4$  Brillouin function, while the sum of  $S = 1/2$  and  $S = 7/2$  Brillouin functions (Figure S3) provides a less than satisfactory agreement with the experimental data. This result suggests that the coupled scenario above provides a more reasonable description of the configuration for  $[\text{K}(2.2.2\text{-cryptand})][\text{Cp}'_3\text{Gd}]$ .

Two other simple cases to consider are  $[\text{K}(2.2.2\text{-cryptand})][\text{Cp}'_3\text{Y}]$  and  $[\text{K}(2.2.2\text{-cryptand})][\text{Cp}'_3\text{La}]$ , both  $S = 1/2$ . For  $\text{Y}^{\text{II}}$ , the unpaired electron will necessarily occupy the 4d shell, and for this ion, as well as  $\text{La}^{\text{II}}$ , experimental evidence suggests that the occupied orbital is  $d_z^2$  in character.<sup>9</sup> Indeed, static magnetic susceptibility data for both compounds collected at 1 T reveal room temperature  $\chi_M T$  values of 0.4 emu·K/mol ( $\text{Y}^{\text{II}}$ ) and 0.37 emu·K/mol ( $\text{La}^{\text{II}}$ ), very close to the theoretical value of 0.375 emu·K/mol expected for an  $S = 1/2$  system (Figure S4). Dc susceptibility data collected at a lower field of 0.1 T also revealed significant temperature-independent paramagnetism in the case of  $\text{Y}^{\text{II}}$  (Figure S4).

The remaining lanthanides can be grouped into two categories, based on the agreement of their experimental  $\chi_M T$  values with those predicted for the  $4f^9 5d^1$  configuration. The first category encompasses  $\text{Tb}^{\text{II}}$ ,  $\text{Dy}^{\text{II}}$ ,  $\text{Ho}^{\text{II}}$ , and  $\text{Er}^{\text{II}}$ , where the

room temperature  $\chi_M T$  values surpass the predicted values for the uncoupled  $4f^9 5d^1$  configuration and closely approach the coupled scenario, in agreement with the results already discussed above for  $\text{Gd}^{\text{II}}$  (Table 1). The lack of perfect agreement might be attributed to the strong crystal field of the  $[\text{Cp}'^-]$  ligand, which could result in incomplete population of the ground  $J$  state at room temperature and/or some quenching of orbital angular momentum; the discrepancy could also very well indicate that this simple model does not sufficiently describe the magnetic properties of these compounds. However, the agreement is still quite good, and the results of the model correspond well with prior experimental data. Notably for  $\text{Dy}^{\text{II}}$  and  $\text{Ho}^{\text{II}}$  (Figure 3), the  $\chi_M T$  values at 300 K

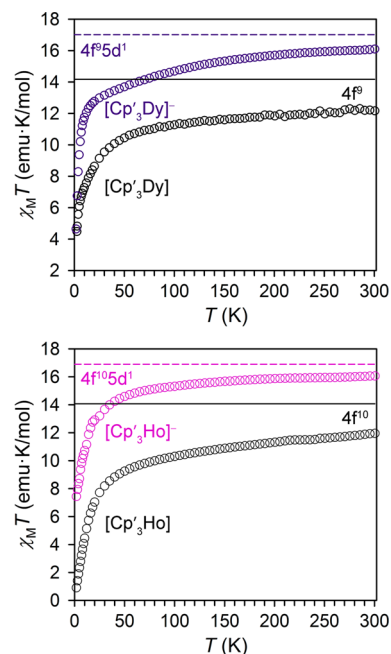


**Figure 3.** Plot of the static magnetic susceptibility times temperature ( $\chi_M T$ ) versus  $T$  for  $[\text{K}(2.2.2\text{-cryptand})][\text{Cp}'_3\text{Dy}]$  (top, purple circles, 1 T) and  $[\text{K}(2.2.2\text{-cryptand})][\text{Cp}'_3\text{Ho}]$  (bottom, pink circles, 0.1 T) along with data for the trivalent analogs under the same respective applied fields (black circles). Dashed colored lines represent the theoretical  $\chi_M T$  value at 300 K assuming the coupled  $4f^9 5d^1$  configuration for each divalent ion, while solid black lines correspond to the theoretical room temperature  $\chi_M T$  value for the corresponding free trivalent ions.

are 16.1 emu·K/mol ( $\mu_{\text{eff}} = 11.35 \mu_B$ ) and 16.26 emu·K/mol ( $\mu_{\text{eff}} = 11.41 \mu_B$ ), respectively. To the best of our knowledge, these represent the highest moments yet exhibited by any metal ion.

A final comment regards the experimental room temperature  $\chi_M T$  value for  $\text{Tb}^{\text{II}}$  (Figure S5, also see for  $\text{Er}^{\text{II}}$ ). While the value of 13.73 emu·K/mol exceeds that expected for the uncoupled  $4f^9 5d^1$  configuration (Table 1), the predicted room temperature  $\chi_M T$  values for the  $4f^9$  and coupled  $4f^9 5d^1$  configuration are 14.13 and 14.42 emu·K/mol, respectively. Thus, the difference between the experimental room temperature  $\chi_M T$  value for  $\text{Tb}^{\text{II}}$  and either of these theoretical possibilities is similar in magnitude to the error between experimental and predicted  $\chi_M T$  for some of the trivalent compounds discussed above. This result again highlights the limitations of such a simple model to describe the magnetic behavior. However, the  $\chi_M T$  data for  $\text{Tb}^{\text{II}}$

are certainly in support of prior experimental evidence suggesting the  $4f^55d^1$  configuration.<sup>9</sup>

The remaining lanthanides,  $\text{Nd}^{\text{II}}$  (Figure 4),  $\text{Ce}^{\text{II}}$ , and  $\text{Pr}^{\text{II}}$  (Figure S6) fall into a distinct category, with room temperature

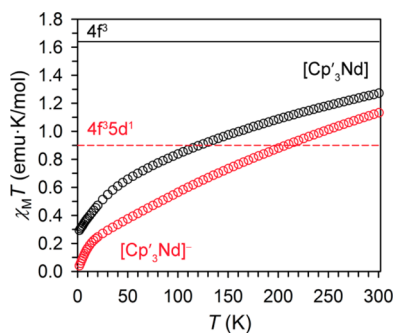


**Figure 4.** Plot of the static magnetic susceptibility times temperature ( $\chi_M T$ ) versus  $T$  collected at 0.1 T for  $[\text{K}(2.2.2\text{-cryptand})][\text{Cp}'_3\text{Nd}]$  and  $\text{Cp}'_3\text{Nd}$ . The room temperature  $\chi_M T$  value for  $\text{Nd}^{\text{II}}$  exceeds that predicted for a  $4f^55d^1$  configuration and also a  $4f^6$  configuration.

$\chi_M T$  values that do not agree well with any of the theoretical categories in Table 1. These values are substantially lower than those predicted for the uncoupled  $4f^55d^1$  configuration, and perhaps based on the  $\text{Gd}^{\text{II}}$  data above, this possibility may therefore be excluded. The experimental values for all three ions actually fall between those predicted for the coupled  $4f^55d^1$  and a  $4f^{n+1}$  configuration. Based on just the  $\chi_M T$  values alone, it is tempting to consider the possibility of a mixed electronic configuration. In the case of  $\text{Nd}^{\text{II}}$ , DFT calculations did suggest that the HOMO contains both d and f character,<sup>9</sup> perhaps adding some credence to this speculation.

Variable-temperature dc susceptibility data collected at higher fields for these three ions indicates that for  $\text{Nd}^{\text{II}}$  and  $\text{Ce}^{\text{II}}$  (both having an even electron count) there is some contribution from temperature-independent paramagnetism (Figure S7), and thus mixing with excited  $J$  states may in part explain the very linear behavior in  $\chi_M T$  as well as the larger than predicted  $\chi_M T$  value at room temperature for these two ions. Indeed, under a field of 1 T, the room temperature  $\chi_M T$  values for  $\text{Ce}^{\text{II}}$  and  $\text{Nd}^{\text{II}}$  are 0.74 and 0.96 emu·K/mol, respectively, closer to (though still larger than) the theoretical values for the coupled  $4f^55d^1$  configuration. In the case of  $\text{Pr}^{\text{II}}$ , dc susceptibility data collected at fields of 0.5 and 1 T exhibited no change from the 0.1 T data, suggesting that temperature-independent paramagnetism is not a significant contribution to the linear  $\chi_M T$  behavior for this compound or the larger than predicted room temperature  $\chi_M T$  value (considering the coupled  $4f^55d^1$  scheme).

## SUMMARY AND CONCLUSIONS

In support of recent spectroscopic and computational results on the series of compounds  $[\text{K}(2.2.2\text{-cryptand})][\text{Cp}'_3\text{Ln}]$ , dc magnetic susceptibility data suggest that a  $4f^n$  configuration is reasonable for  $\text{Sm}^{\text{II}}$ ,  $\text{Eu}^{\text{II}}$ , and  $\text{Tm}^{\text{II}}$ . Conversely, for the remaining paramagnetic later lanthanides, as well as  $\text{Y}^{\text{II}}$  and  $\text{La}^{\text{II}}$ , low-temperature magnetization data ( $\text{Gd}^{\text{II}}$ ) and room temperature  $\chi_M T$  values reveal that a coupled  $4f^55d^1$  configuration is more likely. However,  $\text{Ce}^{\text{II}}$ ,  $\text{Pr}^{\text{II}}$ , and  $\text{Nd}^{\text{II}}$  are outliers, exhibiting dc susceptibility data that do not strongly support either configuration; rather the room temperature  $\chi_M T$  values reveal the severe limitations of such a simple model and

the use of magnetic susceptibility data alone in deciphering electronic structure. The data for these three lanthanides could suggest the interesting possibility of a mixed configuration intermediate between  $4f^55d^1$  and  $4f^{n+1}$ , though additional experiments such as EPR, photoelectron spectroscopy, XAS, and even more refined theory to account for the presence of lanthanide anisotropy are imperative to enabling a more rigorous understanding of these molecules.

Even still, dc susceptibility data reveal exceptionally large room temperature  $\chi_M T$  values and magnetic moments for the later lanthanides, stemming from the  $4f^55d^1$  configuration. In particular,  $\text{Dy}^{\text{II}}$  and  $\text{Ho}^{\text{II}}$  exhibit room temperature magnetic moments that are to our knowledge the highest reported for a single metal ion. Heretofore unheard of, the accessibility of such enormous moments could have intriguing implications in single-molecule magnetism and in the design of new bulk magnet materials. Larger magnetic moments can diminish tunneling of the magnetization<sup>7</sup> in molecular materials, currently one of the major drawbacks in the design of single-molecule magnets with enhanced hysteresis temperatures. Thus, it is interesting to consider that within the proper ligand field symmetry, such accessible moments may enhance single-molecule magnet properties. Bulk magnetic materials are currently limited to early lanthanides such as  $\text{Nd}^{\text{III}}$  or  $\text{Sm}^{\text{III}}$ , an exclusivity that arises from the nature of the magnetic coupling between the f and transition-metal d electrons. For the early lanthanides, the coupling is ferromagnetic, while in the case of the later lanthanides, it is antiferromagnetic; thus, while the anisotropy of the former is smaller, the larger magnetic moments that result from ferromagnetic coupling lead to better permanent magnetic behavior.<sup>5a</sup> If such novel divalent lanthanides were accessible in bulk magnetic materials, the electronic configuration and the larger moments in the case of the later lanthanides could impact both the nature of the magnetic coupling and enhance the overall moment of the material, thus holding promise in the design of new hard permanent magnets with large magnetic energy products.

## ASSOCIATED CONTENT

### Supporting Information

Additional static magnetic susceptibility data. The Supporting Information is available free of charge on the ACS Publications website at DOI: 10.1021/jacs.5b03710.

## AUTHOR INFORMATION

### Corresponding Authors

\*wevans@uci.edu

\*jrlong@berkeley.edu

### Notes

The authors declare no competing financial interest.

## ACKNOWLEDGMENTS

We are grateful to Wayne W. Lukens for helpful discussions and to Matthew R. MacDonald for preliminary sample preparation. This research was supported by NSF Grants CHE-1464841 (J.R.L.) and CHE-1265396 (W.J.E.).

## REFERENCES

- Gatteschi, D.; Sessoli, R.; Villain, J. *Molecular Nanomagnets*; Oxford University Press: Oxford, 2006.
- Nakamura, M.; Ozaki, K.; Hara, S.; Tanaka, M.; Oki, T.; Akai, T.; Watanabe, Y. *AIST Today* 2008, 29, 1.

(3) Croat, J. J.; Herbst, J. F.; Lee, R. W.; Pinkerton, F. E. *J. Appl. Phys.* **1984**, *55*, 2078.

(4) Strnat, K. J.; Hofer, G.; Olson, W.; Ostertag, W.; Becker, J. J. *J. Appl. Phys.* **1967**, *38*, 1001.

(5) (a) Rinehart, J. D.; Long, J. R. *Chem. Sci.* **2011**, *2*, 2078. (b) Woodruff, D. N.; Winpenny, R. E. P.; Layfield, R. A. *Chem. Rev.* **2013**, *113*, 5110. (c) Layfield, R. A. *Organometallics* **2014**, *33*, 1084. (d) Magnani, N. *Int. J. Quantum Chem.* **2014**, *114*, 755. (e) Feltham, H. L. C.; Brooker, S. *Coord. Chem. Rev.* **2014**, *276*, 1. (f) Jiang, S.-D.; Wang, B.-W.; Gao, S. *Advances in Lanthanide Single-Ion Magnets*. In *Molecular Nanomagnets and Related Phenomenon*; Gao, S., Ed.; Springer-Verlag: Berlin, Heidelberg, 2014. (g) Milios, C. J.; Winpenny, R. E. P. *Cluster-Based Single-Molecule Magnets*. In *Molecular Nanomagnets and Related Phenomenon*; Gao, S., Ed.; Springer-Verlag: Berlin, Heidelberg, 2014.

(6) (a) Rinehart, J. D.; Fang, M.; Evans, W. J.; Long, J. R. *Nat. Chem.* **2011**, *3*, 538. (b) Rinehart, J. D.; Fang, M.; Evans, W. J.; Long, J. R. *J. Am. Chem. Soc.* **2011**, *133*, 14236. (c) Demir, S.; Zadrozny, J. M.; Nippe, M.; Long, J. R. *J. Am. Chem. Soc.* **2012**, *134*, 18546.

(7) Considering exclusively tunneling within the ground state at zero applied field and not external factors such as dipolar interactions or symmetry considerations. See: (a) Chudnovsky, E. M.; Tejada, J. *Macroscopic Quantum Tunneling of the Magnetic Moment*; Cambridge University Press: Cambridge, 1998; for example p 33: "...tunneling of large  $S$ , whether due to the anisotropy or due to the field, must always appear in the order of the perturbation theory that scales linearly with  $S$ ." Therefore, for larger  $S$  and magnetic moment, only considering higher orders of perturbation theory will lead to tunneling. From this same reference, the logarithm of the tunneling rate is  $\propto -S$ , which implies a lengthening of the relaxation time or diminishing of tunneling for increasing  $S$ . See also. (b) Gatteschi, D.; Sessoli, R. *Angew. Chem., Int. Ed.* **2003**, *42*, 268. where this rational can be applied directly to spin-only  $\text{Mn}_{12}\text{O}_{12}(\text{CH}_3\text{COO})_{16}$ . For a more specific application to lanthanides: the Landau-Zener tunneling probability gives that with increasing magnitude  $J$  ground state, the tunneling probability decreases. The implicit assumptions here are that the system is axial, with a maximal  $M_J$  ground state and that other factors that might influence tunneling are held constant, such as dipolar interactions or symmetry, see: (c) Urdampilleta, M.; Klyatskaya, S.; Ruben, M.; Wernsdorfer, W. *Phys. Rev. B: Condens. Matter Mater. Phys.* **2013**, *87*, 195412. (d) Wernsdorfer, W.; Sessoli, R.; Caneschi, A.; Gatteschi, D.; Cornia, A.; Mailly, D. *J. Appl. Phys.* **2000**, *87*, 5481. Certainly an axial system with a maximal ground state is not necessary to observe slow relaxation of the magnetization, e.g.: (e) Lucaccini, E.; Sorace, L.; Perfetti, M.; Costes, J.-P.; Sessoli, R. *Chem. Commun.* **2014**, *50*, 1648. However it is usually found to be one of the necessary criteria for slow relaxation under zero applied dc field, through primarily an Orbach mechanism, along with other factors such as collinearity of the ground and first excited-state anisotropy axes, see e.g.: (f) Chilton, N. F.; Langle, S. K.; Moubaraki, B.; Soncini, A.; Batten, S. R.; Murray, K. S. *Chem. Sci.* **2013**, *4*, 1719.

(8) Sugimoto, S. *J. Phys. D: Appl. Phys.* **2011**, *44*, 064001.

(9) (a) MacDonald, M. R.; Bates, J. E.; Ziller, J. W.; Furche, F.; Evans, W. J. *J. Am. Chem. Soc.* **2013**, *135*, 9857. (b) Fieser, M. E.; MacDonald, M. R.; Krull, B. T.; Bates, J. E.; Ziller, J. W.; Furche, F.; Evans, W. J. *J. Am. Chem. Soc.* **2015**, *137*, 369.

(10) The details of the role of crystallography in distinguishing the electron configurations can be found in ref 9b.

(11) Bain, G. A.; Berry, J. F. *J. Chem. Educ.* **2008**, *85*, 532.

(12) Aside from  $\text{Sm}^{\text{II}}$  and  $\text{Tm}^{\text{II}}$ , for which dc susceptibility measurements were highly suggestive of a singlet ground state and strong temperature-independent paramagnetism, respectively. Additionally,  $\text{Cp}'_3\text{Yb}$ , which is isoelectronic with  $\text{Tm}^{\text{II}}$  in this ligand field, exhibited no zero or applied field slow relaxation, precluding the need to measure data for  $\text{Tm}^{\text{II}}$ .

(13) For example: (a) Amberger, H.-D.; Schultze, H.; Edelstein, N. *M. Spectrochim. Acta* **1985**, *41A*, 713. (b) Amberger, H.-D.; Reddmann, H.; Schultze, H.; Jank, S.; Kanellakopulos, B.; Apostolidis, C. *Spectrochim. Acta, Part A* **2003**, *59*, 2527. (c) Red-

dmann, H.; Jank, S.; Schultze, H.; Amberger, H.-D.; Edelstein, N. *Inorg. Chim. Acta* **2003**, *344*, 243. (d) Jank, S.; Reddmann, H.; Amberger, H.-D.; Apostolidis, C. *J. Organomet. Chem.* **2004**, *689*, 3143. (e) Amberger, H.-D.; Reddmann, H.; Liu, G. *J. Organomet. Chem.* **2012**, *716*, 138.

(14) Kahn, O. *Molecular Magnetism*; Wiley-VCH: New York, 1993.

(15) Due to the likely  $4f^{14}$  configuration for  $\text{Yb}^{\text{II}}$  as determined from the characterization in ref 9 and hence diamagnetism expected for  $[\text{K}(2.2.2\text{-cryptand})][\text{Cp}'_3\text{Yb}]$ , the magnetic susceptibility was not measured.

(16) (a) Hitchcock, P. B.; Lappert, M. F.; Maron, L.; Protchenko, A. *V. Angew. Chem., Int. Ed.* **2008**, *47*, 1488. and references therein. (b) Szostak, M.; Procter, D. J. *Angew. Chem., Int. Ed.* **2012**, *51*, 9238.

(17) A  $4f^9 5d^1$  configuration where coupling between the  $f$  and  $d$  electrons is greater than the spin-orbit coupling would also give rise to a predicted room temperature  $\chi_M T = 0$  emu-K/mol. In the case of a  $4f^9 5d^1$  configuration where  $LS$  coupling dominates over spin-coupling (vide supra), still the experimental  $\chi_M T$  value exceeds the predicted 0.47 emu-K/mol. See also: Chilton, N. F.; Goodwin, C. A. P.; Mills, D. P.; Winpenny, R. E. P. *Chem. Commun.* **2015**, *51*, 101–103.

(18) Anderson, D. M.; Cloke, F. G. N.; Cox, P. A.; Edelstein, N.; Green, J. C.; Pang, T.; Sameh, A. A.; Shalimoff, G. *J. Chem. Soc., Chem. Commun.* **1989**, 53. The formal oxidation state of the lanthanide in the benzene and cyclopentadienyl complexes is different; however, the  $\text{Ln}^0$  species were also described with a  $4f^9 5d^1$  configuration, due to full occupation of the  $6s$  orbital with the other two electrons leading to the zero-valent state. One other scenario considered in ref 18 was the case where the additional electron spin couples with the total angular momentum  $J$  of the  $f$  electrons. Such a scenario gives the same predicted  $\chi_M T$  value as the coupled scenario above.